Waste Tire Rubberized Concrete Plates for Airport Pavements: Stress and Strain Profiles in Time and Space Domains

E. Ferretti[1]

Abstract: The present study follows a previous study on the stress and strain profiles along the cross-section of waste tire rubberized concrete plates for airport pavements, subjected to quasi-static loads [Ferretti and Bignozzi (2011, submitted)]. Further results on the in-situ performance of concrete plain and rubberized taxiways have been collected and presented here. The experimental program has been undertaken at the Guglielmo Marconi airport of Bologna (Italy). It concerns two portions of the taxiway, one built with plain concrete and one with rubberized concrete. Each portion has been fitted with strain gauges embedded in concrete for the acquisition of vertical strains.

Keywords: Waste tire rubberized concrete, Elastic half-space, Environmental pollution.

1 Introduction

The rubberization of concrete by means of waste tires is a viable technique in view of the environmental problem related to the recycling of waste tires. The technique is as much attractive as waste tires are a major concern among waste materials: vulcanization processes make tread rubber particularly resistant to the action of microorganisms, which would employ more than 100 years to degrade a tire completely. Thus, the disposal of tires in landfills is impracticable.

A number of techniques have been proposed in the past for recycling waste tires, which allow for their reuse in non-structural elements, both plastic and cementitious elements. In Ferretti and Bignozzi (2011, submitted), recycled waste tires have been used in the mix-design of concrete structural elements for the first time. In particular, the rubberized concrete mixture has been used for preparing a concrete slab to be used in airport pavements. The rubberized concrete was obtained by replacing a 22 Vol.-% of the fine aggregate with rubber scraps, obtained by grinding the tire tread (Fig. 1) and eliminating the metallic fibers of the tread.

Figure 1: Grinding of the tire tread

The idea of using a rubberized cement concrete mixture for airport pavements comes from the comparison of previous results in terms of strength, fatigue resistance, creep, workability and dynamic characteristics of rubberized and plain concrete, by the author and other researchers [Topçu (1995); Fattuhi and Clark (1996); Fedroff, Ahmad, and Savas (1996); Khatib and Bayomy (1999); Wang, Wu, and Li (2000); Hernandez-Olivaresa, Barluenga, Bollatib, and Witoszek (2002); Bignozzi and Sandrolini (2004); Li, Stubblefield, Gregory, Eggers, Abadie, and Huang (2004); Naik and Siddique (2004); Yang, Kim, Lee, Kim, Jeon, and Kang (2004); Bignozzi and Sandrolini (2005); Ghaly and Cahill IV (2005); Bignozzi and Sandrolini (2006); Ferretti and Di Leo (2008); Zheng, Sharon Huo, and Yuan (2008); Topçu and Sarıdemir (2008)]. The main properties that make rubberized concrete eligible for airfield pavements are the ability of absorbing impact energy, reducing or minimizing vibration, and delaying cracking and crushing during fatigue cycles more efficiently than traditional concrete. Indeed fatigue is one of the main causes of distress in airfield pavements, where the repetition is lower but the intensity of loads is greater

[1] DICAM, Facoltà di Ingegneria, Alma Mater Studiorum, Università di Bologna, Viale Risorgimento 2, 40136 (BO), ITALY.

The specimens used for uniaxial compression tests were cylinders of 15 cm (diameter) $\times$ 30 cm (high) and cubes of 15 cm side. They have been prepared in-situ, during concreting (Fig. 17), and cured in laboratory under controlled thermo-hygrometric conditions.

The ratio between cylindrical and cubic strengths was 0.85 for Mixture 1 and 0.80 for Mixture 2.

Fig. 18 shows the stress-strain relationships for two cubic specimens prepared with Mixture 1 and 2, respectively. The 28 days mean compressive strengths and elastic modules for Mixture 1 and 2 (averaged over 3 cubic specimens) are collected in Tab. 2. The decrement in compressive strength when the rubber is added is well evident from both Fig. 18 and Tab. 2. Nevertheless, as discussed in Ferretti and Bignozzi (2011, submitted), it is not essential for airfield applications, since the loads carried by airfield pavements do not overcome the 5% of the collapse load and led the concrete to work in linear-elastic field in both experimental sections.

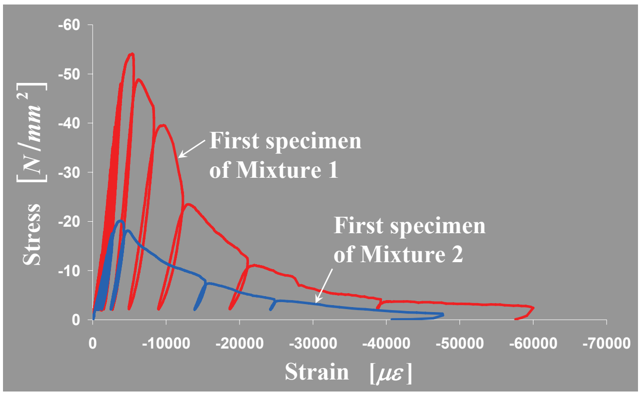

Figure 18: Stress-strain relationships in uniaxial compression for the two mixtures after 28 day curing

The tensile strength has been evaluated by means of Price's empirical method, which provides the ratio between tensile and compressive strength, σ_t and σ_c respectively, as a decreasing function of σ_c (Fig. 19).

From Price's empirical relationship, it follows:

$$\sigma_t = 0.0746\sigma_c = 4.03\,N/mm^2\,, \tag{1}$$

for the first specimen of Mixture 1 (Fig. 19), where $\sigma_c = 54.06\,N/mm^2 = 551\,kg/cm^2$, and

$$\sigma_t = 0.0950\sigma_c = 1.91\,N/mm^2\,, \tag{2}$$

for the first specimen of Mixture 2 (Fig. 19), where $\sigma_c = 20.10\,N/mm^2 = 205\,kg/cm^2$.

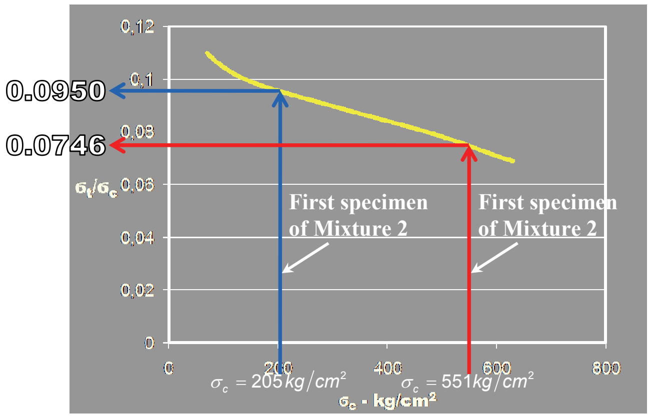

Figure 19: The empirical relationship of Price between the ratio σ_t/σ_c and σ_c

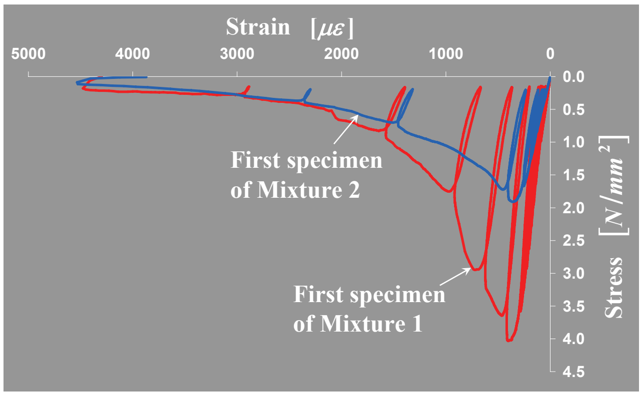

Figure 20: Stress-strain relationships in uniaxial tension for the two mixtures after 28 day curing

Table 2: Mean mechanical properties of Mixture 1 and 2 after 28 day curing (UNI 9416, UNI EN 12390-1:2002, UNI EN 12390-2:2002, UNI EN 12390-3:2003, UNI 6556:1976).

Mixture 1		Mixture 2	
Compressive strength $[N/mm^2]$	Elastic modulus $[N/mm^2]$	Compressive strength $[N/mm^2]$	Elastic modulus $[N/mm^2]$
56.07	13573	20.95	7340

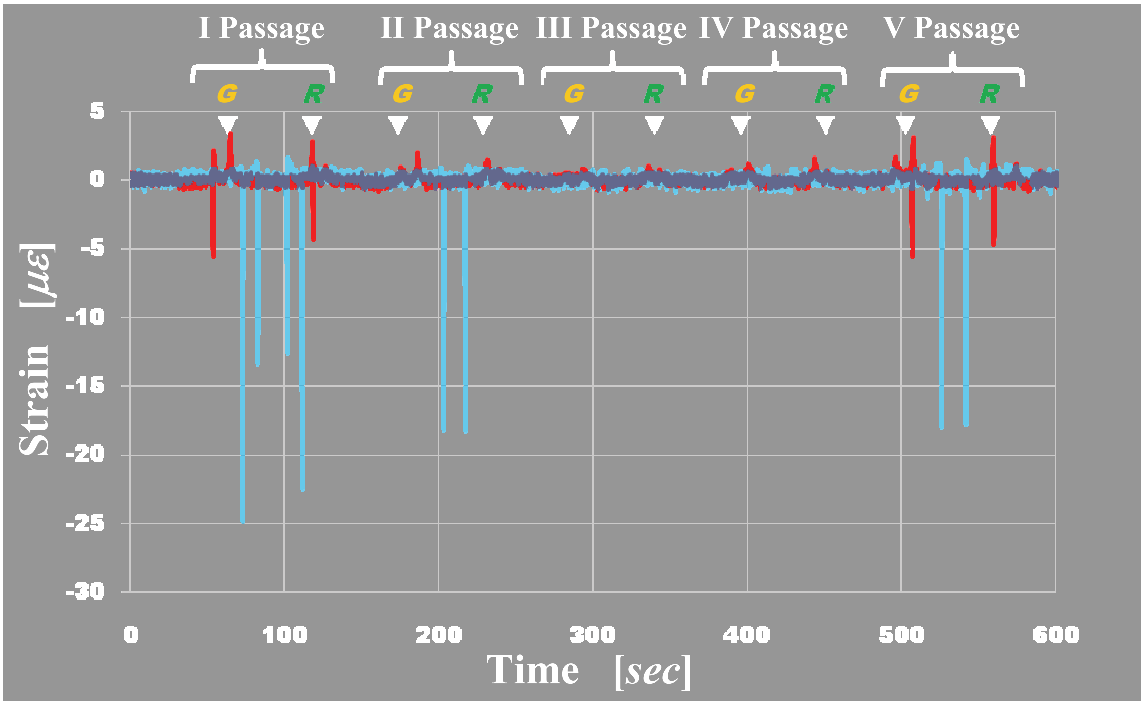

Figure 23: Data acquired by the strain-gauges N° 5 of Section 1 (plain concrete), in red, and 2 (rubberized concrete), in blue

peaks in going are due to the passage of the back wheels (Fig. 24). Moreover, since the return has been made in reverse, the first negative peaks in return are due to the passage of the back wheels, while the second negative peaks in return are due to the passage of the front wheels (Fig. 24). The negative peaks due to the passage of the front wheels are greater than the negative peaks due to the passage of the back wheels, in that the load transmitted by the front wheel is greater than the load transmitted by the back wheels.

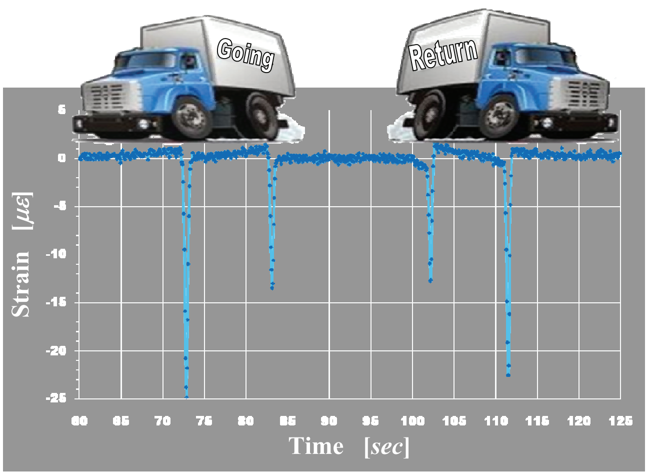

Figure 24: Detail of the first passage over the strain-gauge N° 5 of the second section

Each time a wheel has passed in going over a strain-gauge, both of Section 1 or 2, a recurrent behavior has been observed (see Fig. 25 for Section 2): at first, when the wheel was approaching the strain-gauge, a weak positive strain has appeared in the pavement, then, at the passage of the wheel over the strain-gauge, the strain became negative and reached its maximum absolute value, and finally, when the wheel was leaving the strain-gauge, the strain gradually returned to assume its undisturbed condition value.

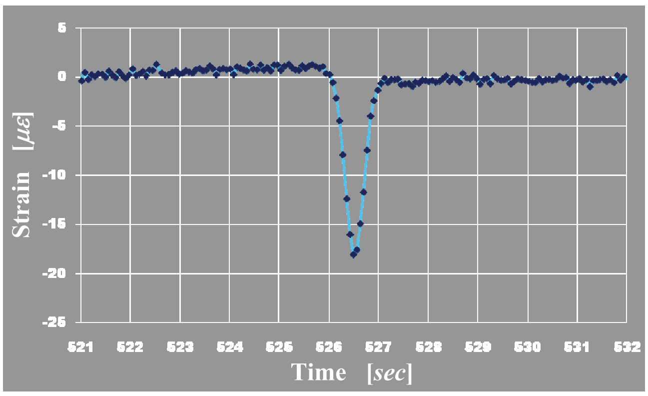

Figure 25: Vertical strain behavior in function of the time when a wheel passes in going over a strain-gauge of the second section

The acquired positive strains do not seem to be caused by friction forces developed at the interface between the pavement and the wheel, since they appear even when the truck speed is very low, that is, in quasi-static conditions. In this last case, the vertical strain profile of Fig. 25 becomes symmetric with respect to the wheel and exhibits two positive peaks of equal intensity, one before and one after the wheel. Consequently, we may conclude that friction is not the main cause of the growing of a positive state of strain inside the pavement, but interacts with it enhancing the positive strains from one side of the wheel and decreasing the positive strains from the other side. In other words, the vertical load has a symmetric effect on the positive strains, while friction has an anti-symmetric effect on them. The behavior of the vertical strain profile along the motion direction comes from the superimposition of these two effects, with the second effect depending on the truck speed.

The increase of tensile stresses when a load moves along a concrete pavement has been assumed by several researchers, in the past [Spangler (1935), Hossain, Muqtadir and Hoque (1997); Darestani, Thambiratnam, Baweja and Nataatmadja (2006)], in order to explain some of the main mechanisms of pavement distress, but never actually experimentally identified inside pavements, to the knowledge of the author. Moreover, since now the tensile stresses induced into pavements by moving loads have always been assumed as longitudinal or transverse stresses (horizontal stresses in both cases). Here, the identified tensile stresses are vertical stresses. Thus, for the first time this work provides an experimental evidence that a tensile state of vertical stress exists in vehicular loaded pavements and provides information on how rubberization acts on it. Actually, in Fig. 23 we can appreciate that, while the negative peaks are greater in rubberized than in plain concrete, due to the greater deformability of rubberized concrete, the opposite happens for positive peaks, which are smaller for rubberized than for plain concrete.

By observing Fig. 23 we can also evaluate the effect of single rather than twin wheels on the tensile state of stress arising into the pavement, since the tensile peaks for the passage of a front single wheel (first peaks in going and second peaks in return) are smaller than the tensile peaks for the passage of a back twin wheel (second peaks in going and first peaks in return), both for Mixture 1 and 2 (for Mixture 2, see the detail in Fig. 24 for major clarity). Thus, the twin wheels interact in a way to enhance the tensile state of stress in concrete pavements, while the compressive state of stress is decreased.

From the knowledge of the truck speed, which has been pre-fixed, it was possible to pass from the time/strain diagrams to the space/strain diagrams. The space/strain diagram associated to Fig. 25 has been plotted in Fig. 26, where the horizontal axis coincides with the motion direction and is positively oriented as the gear direction. In Fig. 26, the positive peak is well evident in front of the wheel.

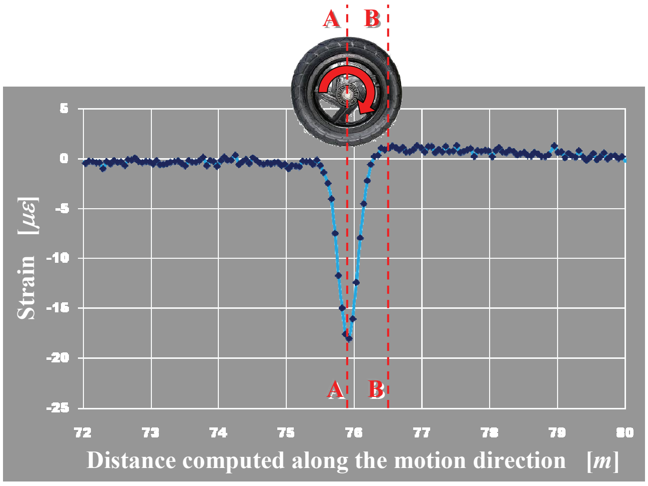

Figure 26: Vertical strain behavior in function of the distance when a wheel passes in going over a strain-gauge of the second section

By comparing the data acquired in the same instant from the five strain-gauges of the same instrumented cross-section, it is possible to build the behavior of strains along each cross-section. The most interesting cross-sections are the ones passing from the compressive and tensile peaks, the **A**-**A** and **B**-**B** sections in Fig. 26 respectively. The behavior of strains along the **A**-**A** cross-section has been already discussed for a front single wheel in Ferretti and Bignozzi (2011, submitted). Here, the strain profile for a front single wheel (Fig. 27) is compared to the strain profile for a back twin wheel (Fig. 28).

As previously pointed out, the maximum strain for twin wheels is lower than the maximum strain for single wheel, due to the lower load transmitted by twin wheels to the pavement. Besides this, the strain profile around the peak is flatter for twin than for single wheels, due to the superimposition of strains induced by both twin wheels. Thus, from the comparison between Figs. 27 and 28 we can conclude that the use of twin instead of single wheels is advantageous as far as the negative state of strain is concerned, since strains are lower and distributed more uniformly on the pavement. Finally, as for single wheels [Ferretti and Bignozzi (2011, submitted)], also for twin wheels strains are spread over a greater area for Mixture 2 than for Mixture 1 (Fig. 28). This means that strain curves of different airfields overlap on a greater portion for Mixture 2 as compared with Mixture 1, limiting the arising of traffic lanes, thus improving the rutting performance of concrete pavements.

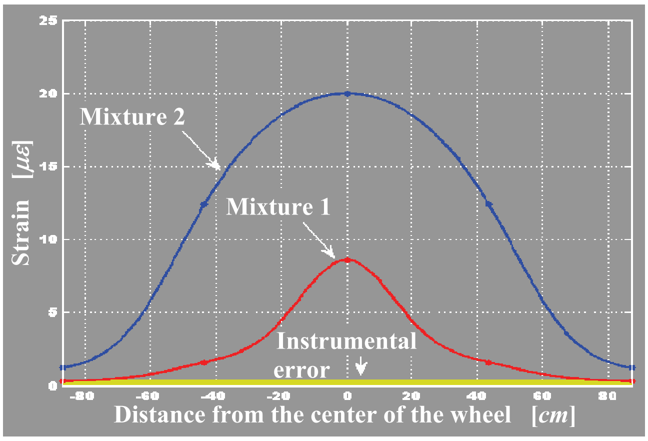

Figure 27: Profiles of vertical strains, in absolute value, induced by the passage of a front single wheel along the **A-A** cross-section

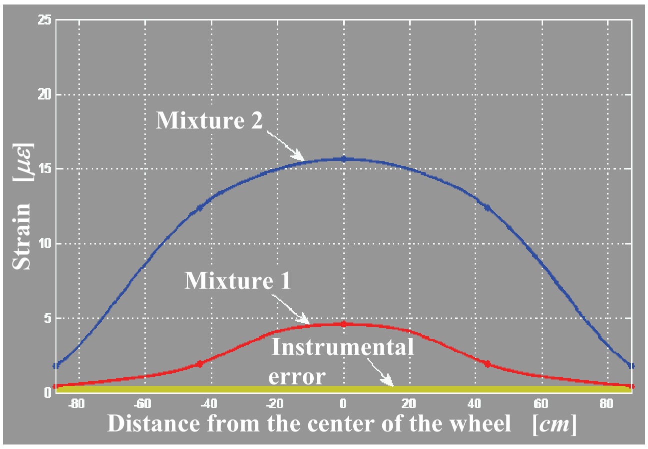

Figure 28: Profiles of vertical strains, in absolute value, induced by the passage of a back twin wheel along the **A-A** cross-section

As far as the behavior of strains along the **B-B** cross-section is concerned, the comparison between the strain profiles plotted for single wheels, in Fig. 29, and twin wheels, in Fig. 30, shows that rubberization is effective in limiting the growth of a tensile state of stress particularly under twin wheels. Actually, the tensile stresses in Section 2, besides being smaller than in Section 1, go to zero more quickly than in Section 1 when they are computed under twin rather than single wheels. Consequently, for twin wheels positive strains are spread over a smaller area for Mixture 2 than for Mixture 1.

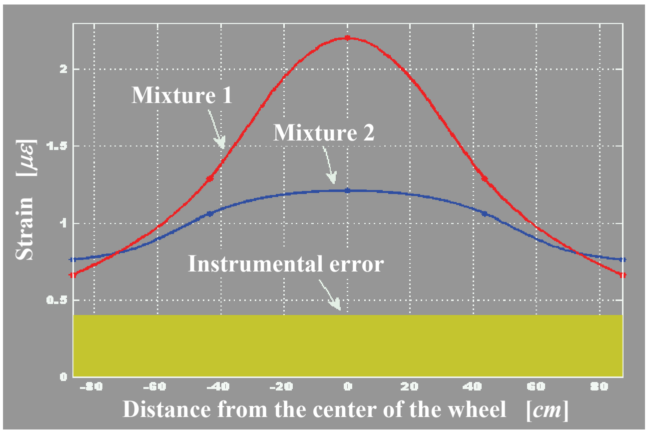

Figure 29: Vertical strain profiles along the **B-B** cross-section induced by the passage of a front single wheel

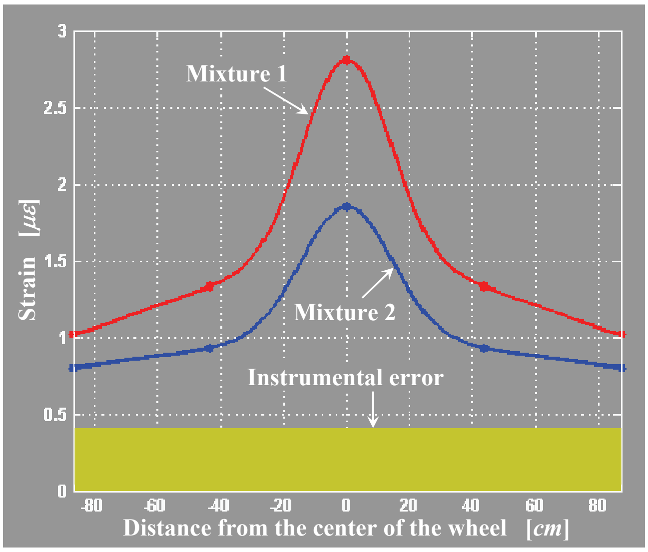

Figure 30: Vertical strain profiles along the **B-B** cross-section induced by the passage of a back twin wheel

Since the involved positive strains are not great enough to make the problem of the permanent strains relevant, the dimension of the positively strained area has not any effect on the rutting performance of concrete pavements. Having a smaller positively strained area means having a lower percentage of pavement surface subjected to strains of opposite sign, alternatively, during the passage of a wheel. Consequently, the use of rubberized instead of plain concrete under twin wheels is advantageous as far as the positive state of strain is concerned, since strains are lower and distributed on a smaller area of the pavement. Since the gear wheels are just twin wheels, this last point gives useful design information to be spent for airfield pavements.

As done in Ferretti and Bignozzi (2011, submitted), the stress profiles have been obtained from the strain profiles in the first-order approximated uniaxial assumption (Eq. 3). As for the stress profiles induced by single wheels along the **A-A** cross-section, discussed in Ferretti and Bignozzi (2011, submitted) and recalled in Fig. (31) for comparison, also in the stress profiles induced by twin wheels along the **A-A** cross-section the peak stress is lower in Mixture 2 than in Mixture 1 (Fig. 32), despite strains are higher for Mixture 2 than for Mixture 1 (Fig. 28). Once more, this happens since k_E, the ratio between E_2, the elastic modulus of Mixture 2, and E_1, the elastic modulus of Mixture 1:

$$k_E = \frac{E_2}{E_1}, \tag{4}$$

is lower than k_ε, the ratio between the peak strains of Mixture 1 and 2, ε_1 and ε_2 respectively:

$$k_\varepsilon = \frac{\varepsilon_1}{\varepsilon_2}. \tag{5}$$

Consequently:

$$\sigma_2 = E_2\varepsilon_2 = k_E E_1 \varepsilon_2 = \frac{k_E}{k_\varepsilon} E_1\varepsilon_1 = \frac{k_E}{k_\varepsilon}\sigma_1 < \sigma_1, \tag{6}$$

where σ_1 is the peak stress in Mixture 1, σ_2 is the peak stress in Mixture 2, and

$$k_E < k_\varepsilon \Rightarrow \frac{k_E}{k_\varepsilon} < 1. \tag{7}$$

Moreover, the stress curve for Mixture 2 is smoother than that of Mixture 1 even for twin wheels. This follows in lower stress gradients for Mixture 2 than for Mixture 1. Since a high stress gradient is one of the main causes of distress for repeated loads, it is reasonable to expect a longer economic life for Mixture 2 than for Mixture 1.

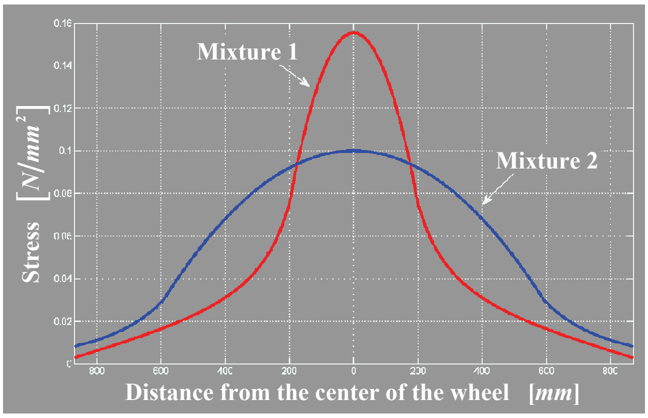

Figure 31: Profiles of vertical stresses, in absolute value, induced by the passage of a front single wheel along the **A-A** cross-section

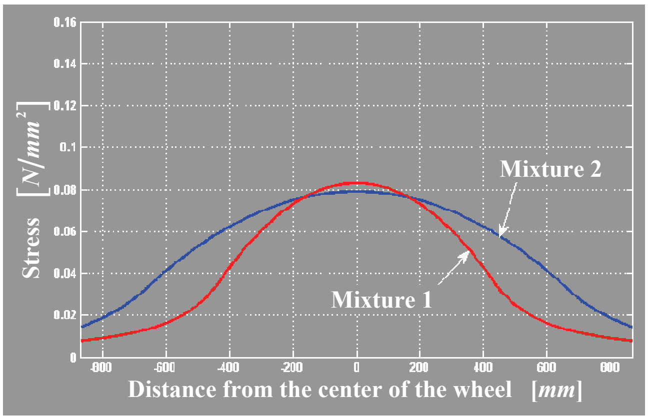

Figure 32: Profiles of vertical stresses, in absolute value, induced by the passage of a back twin wheel along the **A-A** cross-section

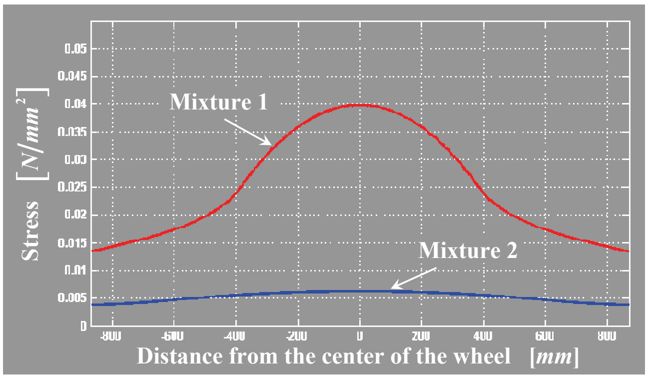

Figure 33: Vertical stress profiles along the **B-B** cross-section induced by the passage of a front single wheel

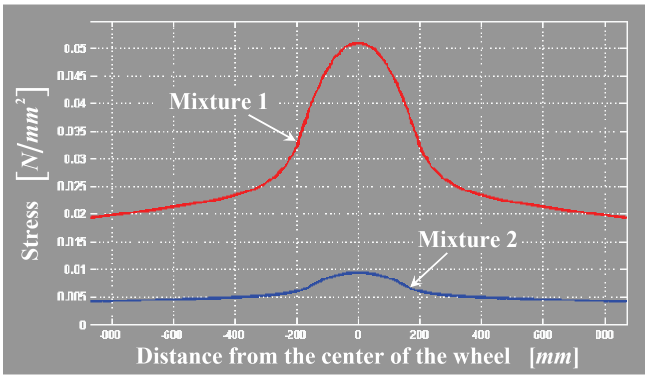

Figure 34: Vertical stress profiles along the **B-B** cross-section induced by the passage of a back twin wheel

The stress profiles along the **B-B** cross-section are shown in Figs. (33), for single wheels, and (34), for twin wheels. Obviously, the advantage connected to the use of rubberized concrete is more evident along the **B-B** cross-section than along the **A-A** cross-section, since strains are already lower for Mixture 2 than for Mixture 1 (Figs. 29 and 30) and, when the stresses are identified from the strains, the ratio between the elastic modules contributes to increase the gap between the curves of plain and rubberized concrete, flatting the curves of rubberized concrete considerably.

From the comparison between Fig. (33), where the involved stresses are positive, and Fig. (31), where the involved stresses are negative, we can conclude that the use of rubberized instead of plain concrete is advantageous for single wheels, since it leads to a reduction (in absolute value) of stresses, both of tensile and compressive nature, and the advantage is much more sensitive for tensile than for compressive stress profiles. The same can be concluded for twin wheels, from the comparison between Figs. (34) and (32). It is worth noting that having a decreased state of tensile stress is particularly remarkable, since just tensile stresses induced by moving loads are one of the main causes of premature distress of concrete pavements.

By interpolating the stress profiles both along the motion direction and the cross-sections, it was possible, finally, to obtain the stress behavior under the wheel-print for plain (Fig. 35) and rubberized concrete (Fig. 36).

4 Conclusions

A rubberized cement concrete mixture has been used for preparing a concrete slab customarily used for rigid pavements, but the subbase and subgrade courses were those typical of a flexible pavement and the concrete slab thickness was much smaller than that of a rigid pavement. A second slab has been prepared with a control plain concrete mixture, for comparison purposes. Both slabs have been fitted with strain-gauges embedded in concrete very near to the slab surface, in order to investigate the complex state of vertical strain of the superficial pavement layers and identify the related vertical stress field. Moreover, having used a truck pro-

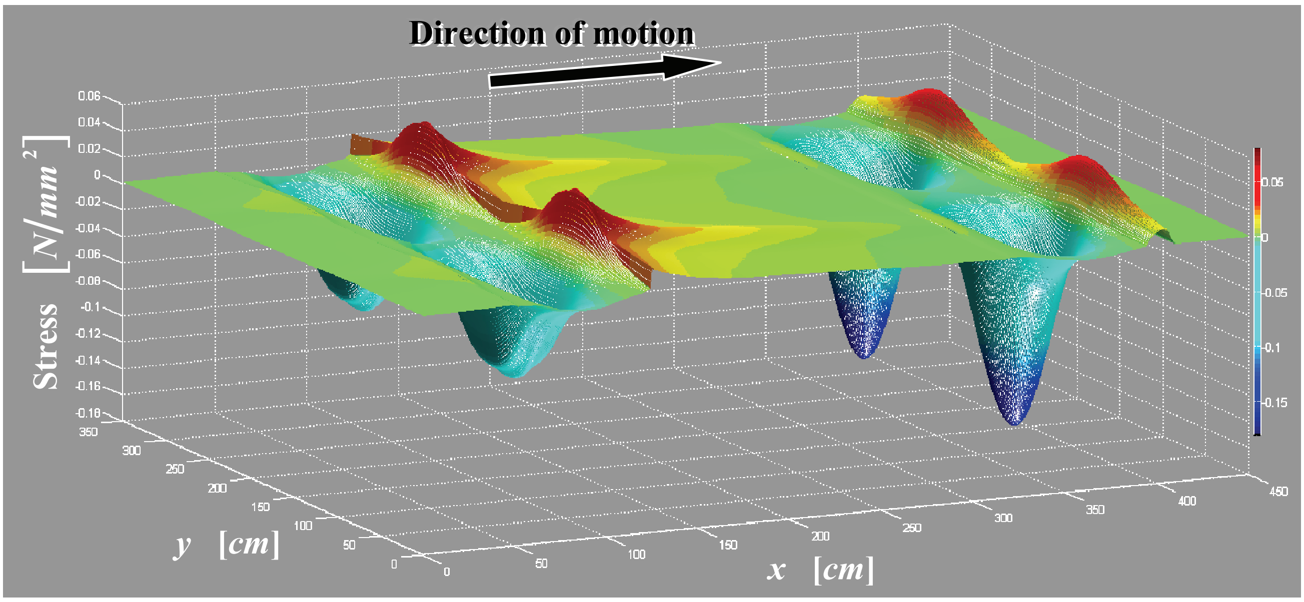

Figure 35: Vertical stresses under the wheel-print for plain concrete

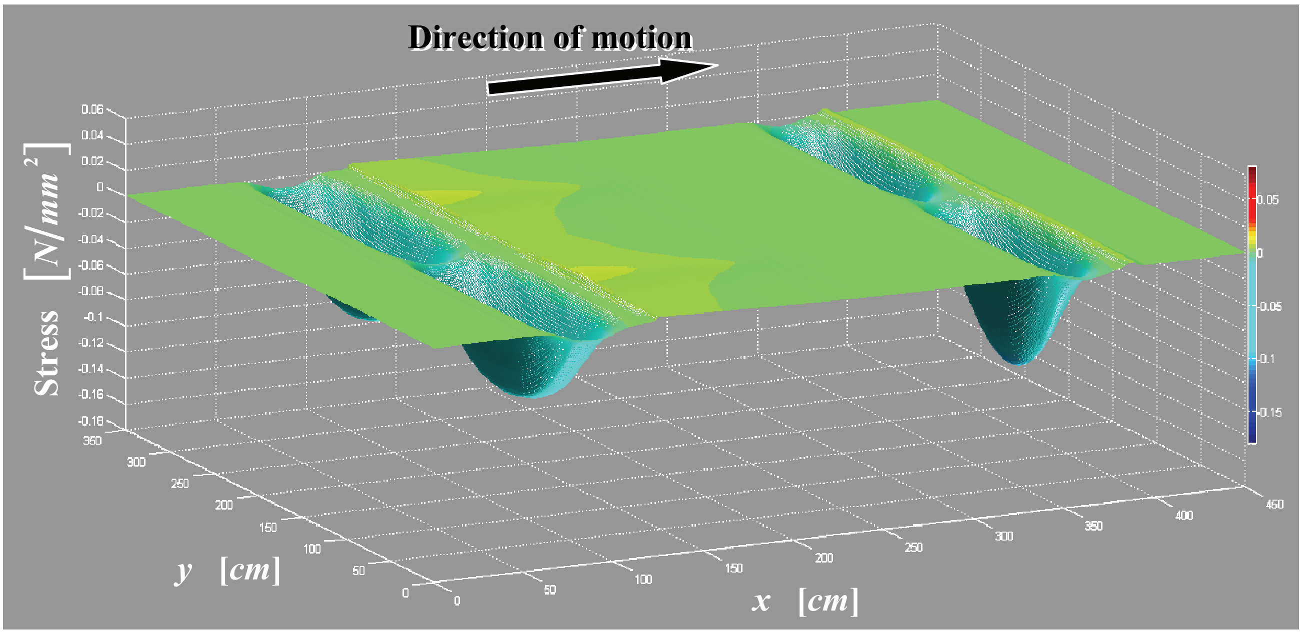

Figure 36: Vertical stresses under the wheel-print for rubberized concrete

vided of both single and twin wheels as mobile load, it was possible to estimate the effect of the wheel configuration on the induced vertical strains and stresses.

One of the main results of the experimentation concerns the identification of a tensile state of vertical stress induced into the pavement by mobile loads, since the existence of tensile vertical stresses has been never experimentally verified previously. Since tensile stresses must be kept as low as possible in concrete, it is of primary importance to evaluate how the use of a rubberized instead of a plain concrete mixture or single instead of twin wheels acts on them. It has been found that twin wheels act negatively on the tensile state of stress, enhancing it, while rubberization acts positively, reducing it. Twin wheels are used more and more frequently, due to the constant growth of aircraft dimensions, and constitute the major part of gear wheels. This makes the ability of decreasing tensile stresses of rubberized concrete particularly interesting.

When coupled with twin wheels, rubberized concrete is effective also in decreasing the peak compressive vertical stress and increasing the rutting performance of concrete pavements. Thus, we may conclude that rubberization ameliorates the performance of concrete pavements as far as its behavior both in tension and compression.

The choice of a Mixture instead of another cannot be based on the stress field induced into mixtures by load exclusively, of course. The stress field must be related to the compressive and tensile strength of mixtures, before deciding what mixture to use. Nevertheless, since the involved stresses are very far from the compressive and tensile strength for both Mixtures, the difference between compressive strengths in plain and rubberized concrete, from one hand, and tensile strengths in plain and rubberized concrete, on the other hand, can be neglected. This means that the choice may be done by comparing Figs. 35 and 36 directly, with the criterion of preferring the Mixture giving the lower state of tensile stress when loaded by vehicular traffic. As can be checked in Figs. 35 and 36 easily, the mixture satisfying this criterion is the rubberized one.

5 Future developments

The tensile state of stress identified into the pavement is not justified by Boussinesq's closed elastic solution for a homogeneous, linear-elastic and isotropic half-space subjected to a point-load perpendicular to the surface [Boussinesq (1876); Boussinesq (1885)], directly or indirectly used for airfield pavement design. Neither are more refined models and empirical methods [Fröhlich (1934); Burmister (1943); Westergaard (1943); Odemark, (1949); Söehne (1958); Veverka, (1973); Binger and Wells (1989); Sharifat and Kushwaha (2000); Barker and Gonzalez, (2006); Gonzales (2006); Seyrafian, Gatmiri and Noorzad (2007); Caron, Theillout and Brill (2010)] able to account for tensile stresses.

In Ferretti and Bignozzi (2011, submitted), it was already pointed out how Boussinesq's closed elastic solution does not provides information even on the relationship between the elastic parameters of the medium and the stress profiles along the cross-section, relationship which has been experimentally verified just in Ferretti and Bignozzi (2011, submitted). Since the existence of tensile stresses is actually compatible with some distress mechanisms of concrete pavements, the present experimentation, together with the findings of Ferretti and Bignozzi (2011, submitted), seem to suggest a revision of Boussinesq's closed elastic solution. This may lead to a better comprehension of the stress field induced by an aircraft to airfield pavements. In particular, it may clarify the mechanism of stress transfer near the surface for static and dynamic loads, that seems not to be sufficiently exploited at present, as extensively discussed in Ferretti and Bignozzi (2011, submitted). In perspective, the enhanced theory of Boussinesq may lead to formulate a more realistic criterion of design for airfield pavements, which better accounts for stresses and deflections than the methods currently used.

Acknowledgment The SAB staff – infrastructures development, Guglielmo Marconi Airport of Bologna (Italy), and, especially, Domenico Terra, Engineer, are gratefully acknowledged for having assigned the taxiway of the airport to the experimentation of the new proposed airfield pavement. Eng. Adriano Cirasole is also acknowledged for his active contribution in data processing.

References

Barker, W.R. and Gonzalez, C.R. (2006): *Independent Evaluation of 6-Wheel Alpha Factor Report*. Letter Report to the Federal Aviation Administration, U.S. Army Engineer Research and Development Center, Vicksburg, Mississippi.

Bignozzi, M.C. and Sandrolini, F. (2004): Recycling tyre rubber in building materials. Proc. *International Conference: Sustainable Waste Management and Recycling: Used/Post-Consumer Tyres*, Kingston University, London, September 14–15 2004, Thomas Telford, London, pp. 77–84.

Bignozzi, M.C. and Sandrolini, F. (2005): Il riciclo di pneumatici particellati come aggregati fini in malte cementizie auto compattanti. Proc. *Seminari di Ecomondo 2005*, Maggioli Editore, 26-29 Ottobre 2005, Rimini, pp. 41–46.

Bignozzi, M.C. and Sandrolini, F. (2006): Tyre rubber waste recycling in self-compacting concrete. *Cement Concrete Res*., vol. 36, pp. 735–739.

Binger, R.L. and Wells, L.G. (1989): *Simulation of compaction from surface mining systems*. ASAE Paper no. 89-2018, St. Joseph, MI: ASAE.

Boussinesq, M.J. (1876): *Essai théorique sur l'équilibre d'élasticité des massifs pulvérulents compare à celui de massifs solides et sur la poussée des terres sans cohésion*. Mémoires des Savants Etrangers, Académie de Belgique, 40, Bruxelles.

Boussinesq, M.J. (1885): *Application des potentiels a l'étude de l'équilibre et du mouvement des solides élastiques, avec des notes étendues sur divers points de physique mathématique et d'analyse*. Gauthier-Villars imprimeur libraire, Paris.

Burmister, D. M. (1943): The Theory of Stresses and Displacements in Layered Systems and Applications to the Design of Airport Runways. Proc. *Highway Research Board*, vol. 23.

Caron, C., Theillout, J.N. and Brill, D.R. (2010): Comparison of US and French Rational Procedures for the Design of Flexible Airfield Pavements. Proc. *2010 FAA Worldwide Airport Technology Transfer Conference*, Atlantic City, New Jersey, USA, April 2010, 23 pp.

Darestani, M.Y., Thambiratnam, D.P., Baweja, D. and Nataatmadja, A. (2006): Dynamic Response of Concrete Pavements under Vehicular Loads. *Proceedings IABSE Symposium*, Budapest, Hungary, 2006, 8 pp.

Fattuhi, N.I. and Clark, L.A. (1996): Cement-based materials containing shredded scrap truck tyre rubber. *Constr. Build. Mater*., vol. 10, no. 4, pp. 229–236.

Fedroff, D., Ahmad, S. and Savas, B.Z. (1996): Mechanical properties of concrete with ground waste tire rubber. *Transportation Research Board 1996; Report No. 1532*, pp. 66–72.

Ferretti, E. and Bignozzi, M.C. (2011 submitted): Stress and Strain Profiles along the Cross-Section of Waste Tire Rubberized Concrete Plates for Airport Pavements. *CMC – Comput. Mater. Con.*

Ferretti, E. and Di Leo, A. (2008): Cracking and Creep Role in Displacement at Constant Load: Concrete Solids in Compression. *CMC – Comput. Mater. Con.*, vol. 7, no. 2, pp. 59–80.

Fröhlich, O.K. (1934): *Druckverteilung im Baugrunde*. Springer Verlag, Wien.

Ghaly, A.M. and Cahill IV, J.D. (2005): Correlation of strength, rubber content, and water to cement ratio in rubberized concrete. *Can. J. Civil. Eng*., vol. 32, no. 6, pp. 1075–1081.

Gonzales, C.R. (2006): Implementation of a New Flexible Pavement Design Procedure for U.S. Military Airports. Proc. *Fourth LACCEI International Latin American and Caribbean Conference for Engineering and Technology* (LACCEI'2006), Mayagüez, Puerto Rico, 21-23 June 2006, 2006, 10 pp.

Hernandez-Olivaresa, F., Barluenga, G., Bollatib, M. and Witoszek, B. (2002): Static and dynamic behaviour of recycled tyre rubber-filled concrete. *Cement Concrete Res*., vol. 32, no. 10, pp. 1587–1596.

Hossain, M., Muqtadir, A. and Hoque, A.M. (1997): Three-Dimensional Finite Element Analysis of Concrete Pavement System. *Journal of Civil Engineering*, the Institution of Engineers, Bangladesh, vol. CE 25, No. 1, pp. 33–47.

Khatib, Z.K. and Bayomy, F.M. (1999): Rubberized Portland cement concrete. *J. Mater. Civil. Eng*., vol. 11, no. 3, pp. 206–213.

Li, G.Q., Stubblefield, M.A., Gregory, G., Eggers, J., Abadie, C. and Huang, B.S. (2004): Development of waste tire modified concrete. *Cement Concrete Res*., vol. 34, no. 12, pp. 2283–2289.

Naik, T.R. and Siddique, R. (2004): Properties of concrete containing scrap tire rubber – an overview. *Waste Manage*, vol. 24, no. 6, pp. 563–569.

Odemark, N. (1949): *Undersökning av elasticitetegenskaperna hos olika jordarter samt teori för beräkning av belägningar enligt elasticitetsteorin*. Statens Väginstitut, meddelande 77.

Seyrafian, S., Gatmiri, B. and Noorzad, A. (2007): Analytical Investigation of Depth Non-homogeneity Effect on the Dynamic Stiffness of Shallow Foundations. *CMES – Comp. Model. Eng.*, vol. 21, no. 3, pp. 209–217.

Sharifat, K. and Kushwaha, R. L. (2000): *Modeling soil movement by tillage tools*. Saskatoon, Saskatchewan Canada: Department of Agricultural and Bioresource Engineering, University of Saskatchewan.

Söehne, W. (1958): Fundamentals of pressure distribution and soil compaction under tractor tires. *Agricultural Engineering*, vol. 39, pp. 276–281.

Spangler, M.G. (1935): Stresses in Concrete Pavement Slabs. *Transportation Research Board of the National Academies – Highway Research Board Proceedings*, vol. 14, No. Pt1.

Topçu, İ.B. (1995): The properties of rubberized concretes. *Cement Concrete Res*., vol. 25, no. 2, pp. 304–310.

Topçu, İ.B. and Sarıdemir, M. (2008): Prediction of rubberized concrete properties using artificial neural network and fuzzy logic. *Construction Build. Mater.*, vol. 22, pp. 532–540.

Veverka, V. (1973): *Modules, contraintes et déformations des massifs et couches granulaires*. Rapport de Recherche, no. 162, vv, Centre de Recherches Routières, Bruxelles.

Wang, Y., Wu, H.C. and Li, V.C. (2000): Concrete reinforcement with recycled fibers. *J. Mater. Civil. Eng*., vol. 12, no. 4, pp. 314–319.

Westergaard, H.M., (1943): New Formulas for Stresses in Concrete Pavements of Airfields. *ACE Transactions*, vol. 108. Also in *ACE Proceedings*, vol. 73, no. 5, May, 1947.

Yang, H.S., Kim, D.J., Lee, Y.K., Kim, H.J., Jeon, J.Y. and Kang, C.W. (2004): Possibility of using waste tire composites reinforced with rice straw as construction materials. *Bioresource Technol.*, vol. 95, pp. 61–65.

Zheng, L., Sharon Huo, X. and Yuan, Y. (2008): Experimental investigation on dynamic properties of rubberized concrete. *Constr. Build. Mater*., vol. 22, pp. 939–947.